Direct electron transfer-type bioelectrocatalysis by membrane-bound aldehyde dehydrogenase from Gluconobacter oxydans and cyanide effects on its bioelectrocatalytic properties

AUTHOR(S):

Adachi, Taiki; Kitazumi, Yuki; Shirai, Osamu; Kano, Kenji

CITATION:

Adachi, Taiki ...[et al]. Direct electron transfer-type bioelectrocatalysis by membrane-bound aldehyde dehydrogenase from Gluconobacter oxydans and cyanide effects on its bioelectrocatalytic properties. Electrochemistry Communications 2021, 123: 106911.

ISSUE DATE:

2021-02

URL:

http://hdl.handle.net/2433/276835

Electrochemistry Communications 123 (2021) 106911

Contents lists available at ScienceDirect

Electrochemistry Communications

journal homepage: www.elsevier.com/locate/elecom

Full Communication

Direct electron transfer-type bioelectrocatalysis by membrane-bound aldehyde dehydrogenase from *Gluconobacter oxydans* and cyanide effects on its bioelectrocatalytic properties

Taiki Adachi, Yuki Kitazumi *, Osamu Shirai, Kenji Kano *

Division of Applied Life Sciences, Graduate School of Agriculture, Kyoto University, Sakyo, Kyoto 606-8502, Japan

ARTICLE INFO

Keywords:
Membrane-bound aldehyde dehydrogenase
Bioelectrocatalysis
Direct electron transfer
Acetaldehyde oxidation
Cyanide coordination

ABSTRACT

The bioelectrocatalytic properties of membrane-bound aldehyde dehydrogenase (AlDH) from *Gluconobacter oxydans* NBRC12528 were evaluated. AlDH exhibited direct electron transfer (DET)-type bioelectrocatalytic activity for acetaldehyde oxidation at several kinds of electrodes. The kinetic and thermodynamic parameters for bioelectrocatalytic acetaldehyde oxidation were estimated based on the partially random orientation model. Moreover, at the multi-walled carbon nanotube-modified electrode, the coordination of CN^- to AlDH switched the direction of the DET-type bioelectrocatalysis to acetate reduction under acidic conditions. These phenomena were discussed from a thermodynamic viewpoint.

1. Introduction

Acetic acid bacteria have a variety of membrane-bound dehydrogenases that work in their unique metabolism such as acetic acid fermentation [1]. The application of these bacteria in bioelectrochemical devices (biosensors, biofuel cells, biosupercapacitors, etc.) is significant for industry [1]. Specifically, membrane-bound dehydrogenases such as fructose dehydrogenase (FDH) [2], alcohol dehydrogenase (ADH) [3–5], gluconate dehydrogenase (GaDH) [6], and lactate dehydrogenase (LDH) [7] are known to directly communicate with electrodes and proceed electro-enzymatic reactions, which is called direct electron transfer (DET)-type bioelectrocatalysis. It is suggested that these dehydrogenases transfer electrons from their substrates to the electrodes via their catalytic centers and one or more hemes *c* in this order [1].

Herein, we focus on another membrane-bound dehydrogenase of acetic acid bacteria, namely, aldehyde dehydrogenase (AlDH). AlDH from *Gluconobacter oxydans* NBRC12528 is a heterotrimeric enzyme composed of a large subunit (86 kDa) containing a molybdopterin cofactor (Moco) as a catalytic center, a membrane-bound cytochrome *c* subunit (55 kDa) containing three hemes *c*, and a small subunit (the molecular mass of which is unknown) containing an iron-sulfur cluster [8,9]. In vivo, AlDH oxidizes acetaldehyde, and the extracted electrons are transferred to ubiquinone in the inner membrane [9]. However, the electrochemical properties and the bioelectrocatalytic performance of AlDH have not yet been examined.

In the present study, we report DET-type bioelectrocatalysis by AlDH at planar gold (Au), 2-mercaptoethanol (ME)-functionalized Au, and multi-walled carbon nanotube (MWCNT)-modified glassy carbon (GC) electrodes. Planar and ME-functionalized Au electrodes were used as platforms for DET-type bioelectrocatalysis by FDH [2,10]. MWCNTs are nanostructured electrode materials that promote various DET-type reactions [11] with the following effects: 1) the enlarged effective surface area of the electrode increases the amount of adsorbed enzymes [12]; 2) the curvature of the mesoporous electrode structure increases the probability of enzyme orientations suitable for DET-type reactions [13,14]; 3) the electric field strengthened by the expansion of the electric double layer accelerates the kinetics of heterogeneous electron transfer at the edge of the micropores [15].

The effects of the coordination of cyanide ions (CN^-) to the hemes *c* on the bioelectrocatalytic properties of AlDH are also evaluated herein. Interestingly, CN^--coordinated AlDH exhibits DET-type activity for acetate reduction.

* Corresponding authors.
E-mail addresses: kitazumi.yuki.7u@kyoto-u.ac.jp (Y. Kitazumi), kano.kenji.5z@kyoto-u.ac.jp (K. Kano).

https://doi.org/10.1016/j.elecom.2020.106911
Received 1 December 2020; Received in revised form 21 December 2020; Accepted 23 December 2020
Available online 29 December 2020

2. Experimental

2.1. Materials and chemicals

Protein markers for sodium dodecyl sulfate polyacrylamide gel electrophoresis (SDS-PAGE) were obtained from Nacalai Tesque Inc. (Japan). Water-dispersed MWCNTs were kindly donated by Nitta Co. (Japan). Other reagents were purchased from Wako Pure Chemical Industries, Ltd. (Japan). All solutions were prepared using ultrapure water.

2.2. Purification of AlDH

AlDH was purified from a variant of *Gluconobacter oxydans* NBRC12528 (Δ*adhA*::Km^r [16]) according to the procedure in the literature [8], with minor modifications. Briefly, the process of removing ADH from the membrane fraction using multiple surfactants was omitted because the gene of ADH was knocked out. The purified enzyme solution contained 0.5% Triton® X-100 as a solubilizer and 25 mM benzaldehyde and 10% sucrose as stabilizers. The results of SDS-PAGE analysis are shown in Fig. S1, which demonstrate that the subunit structure of AlDH from the variant was identical to the reported structure of that purified from the wild-type cells [8].

The AlDH activity was spectrophotometrically measured using potassium ferricyanide as an electron acceptor and ferric sulfate-Dupanol reagent [8]. Here, one unit (U) of AlDH activity is defined as the amount of the enzyme that oxidizes 1 μmol of acetaldehyde per minute at pH 4.0. The protein concentration was estimated using a DC protein assay kit (Bio-Rad, USA) with bovine serum albumin as the standard. The specific activity (approximately 600 U mg^{-1}) was slightly better than that described in the literature (430 U mg^{-1} [8]), plausibly due to the shortening of the purification process, as described above.

2.3. Electrode preparation

Au and GC electrodes (3 mm in diameter, BAS, Japan) were polished with 1.0 μm and 0.05 μm alumina powder. The electrodes were subsequently rinsed by sonication in distilled water. Self-assembled monolayers of 2-mercaptoethanol (ME) were then formed on the Au electrodes by immersing the Au electrodes in an ethanol solution containing 2 mM ME for 2 h. Subsequently, the ME-functionalized Au electrodes were washed with ethanol and distilled water. MWCNT-modified GC electrodes were also prepared by applying 60 μL of 0.1 wt% MWCNT dispersion to the surface of each GC electrode, followed by drying at 70 °C.

2.4. Electrochemical measurements

All electrochemical measurements were performed at 25 °C with electrochemical analyzers (CV-50 W (BAS, USA) or ALS 701E (ALS Co. Ltd., Japan)). Anaerobic measurements were carried out in a nitrogen (N_2) chamber filled with a mixture of 96% N_2 and 4% H_2. A platinum wire and a homemade Ag|AgCl|sat. KCl electrode were used as the counter and reference electrodes, respectively. In this study, all potentials are referred to the reference electrode.

3. Results and discussion

3.1. DET-type bioelectrocatalytic acetaldehyde oxidation by AlDH

Fig. 1 shows cyclic voltammograms (CVs) recorded at planar and ME-functionalized Au electrodes in a McIlvaine buffer (McB) (pH 4.0) containing 0.1 M acetaldehyde under Ar atmospheric conditions. After adding AlDH at a final concentration of 2 μg mL^{-1} into the electrolysis solution, clear sigmoidal waves were observed at both electrodes (Fig. 1A). As shown in Fig. S2, the anodic current density gradually increased with time and finally reached the maximum value. Thus, these waves are ascribed to DET-type bioelectrocatalysis of acetaldehyde oxidation by AlDH physically adsorbed on the electrodes. The bioelectrocatalytic current density reached approximately 20 μA cm^{-2} at the planar Au electrode and 30 μA cm^{-2} at the ME-functionalized Au electrode at 0.4 V. On the other hand, the slightest anodic current was also observed in the absence of acetaldehyde (Fig. S3), which seems to be due to the DET-type oxidation of benzaldehyde contained in an enzyme solution.

In this study, kinetic and thermodynamic analysis of the DET-type bioelectrocatalytic waves at the AlDH-modified electrodes was performed using a partially random orientation model in which it was assumed that the enzymes were adsorbed on the electrode surface in a homogeneously distributed orientation [17,18]. In the model, the steady-state current density (j) is expressed by the following equation [17]:

$$j = \frac{j_{cat}}{\beta\Delta d(1+\eta^{-1})} \ln\left|\frac{\frac{k^{\circ}_{max}}{k_c}(1+\eta)+\eta^{\alpha}}{\frac{k^{\circ}_{max}}{k_c}(1+\eta)\exp(-\beta\Delta d)+\eta^{\alpha}}\right| \quad (1)$$

where j_{cat} is the limited steady-state catalytic current density, k°_{max} is

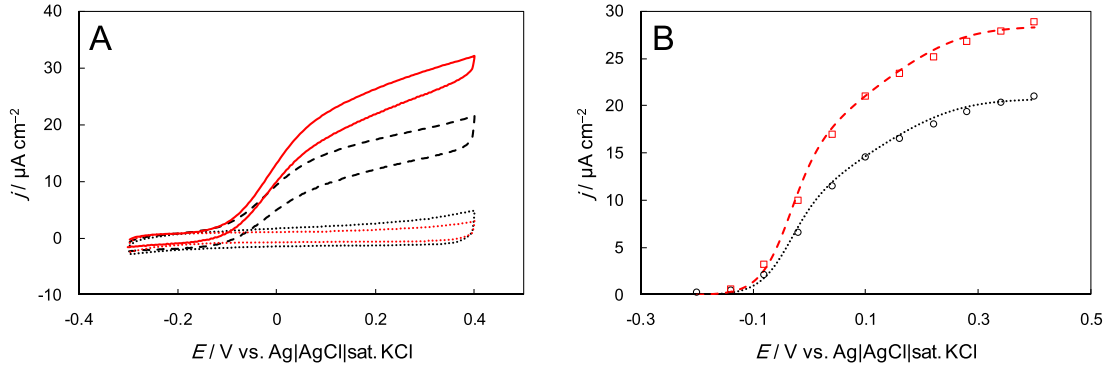

Fig. 1. (A) CVs for acetaldehyde oxidation at the AlDH-modified planar Au electrode (broken black line) and ME-functionalized Au electrode (solid red line) in an McB (pH 4.0) containing 0.1 M acetaldehyde and 2 μg mL^{-1} AlDH at 25 °C under quiescent and Ar atmospheric conditions, at a scan rate (v) of 10 mV s^{-1}. CVs in the absence of AlDH are represented by dotted lines. (B) Background-subtracted linear sweep voltammogram for acetaldehyde oxidation at the AlDH-modified planar Au electrode (black circles) and ME-functionalized Au electrode (red squares) in an McB (pH 4.0) containing 0.1 M acetaldehyde and 2 μg mL^{-1} AlDH at 25 °C under quiescent and Ar atmospheric conditions, at $v = 10$ mV s^{-1}. The dotted and broken lines indicate the refined curves estimated by non-linear regression analysis based on Eq. (1). (For interpretation of the references to colour in this figure legend, the reader is referred to the web version of this article.)

the standard rate constant for heterogeneous electron transfer between the electrode and the redox center of AlDH in the best orientation, k_c is the catalytic constant, Δd is the difference in the distance between the closest and farthest approaches of the redox center of AlDH that electrochemically communicates with an electrode, α is the transfer coefficient (assumed to be 0.5 in this case), and β is the decay coefficient of long-range electron transfer (assumed to be 1.4 Å $^{-1}$ for proteins [19]). In addition, j_{cat} and η are given as follows:

$$j_{cat} = n_S F k_c \Gamma_{E,eff} \quad (2)$$

$$\eta = \exp\left\{\frac{n'_E F}{RT}\left(E - E^{\circ\prime}_E\right)\right\} \quad (3)$$

where n_S is the number of electrons in acetaldehyde oxidation (=2), n'_E is the number of electrons in the rate-determining step of the heterogeneous electron transfer (=1 in general), $\Gamma_{E,eff}$ is the surface concentration of the effective enzyme immobilized on the electrode, E is the electrode potential, $E^{\circ\prime}_E$ is the formal potential of the electrode-active redox center of AlDH, F is the Faraday constant, R is the gas constant, and T is the absolute temperature. Using $E^{\circ\prime}_E$, k°_{max}/k_c, Δd, and j_{cat} as adjustable parameters, Eq. (1) was fitted to the steady-state catalytic waves using non-linear regression analysis with Gnuplot. The background currents were subtracted from the total currents before analysis. The fitting results are shown in Fig. 1B, and the refined numerical data are summarized in Table 1. The errors are due to the variation in the characteristics of enzyme-modified electrodes.

The $E^{\circ\prime}_E$ values seem to be assigned to the electrode-active heme *c*, as compared to the spectrophotometrically determined values of the formal potentials of hemes *c* in FDH ($E^{\circ\prime}$ = 150 mV, 60 mV, and −10 mV) [20]. The value of $E^{\circ\prime}_E$ appeared to be independent of the surface modification of the Au electrode. In addition, there was no significant difference in the estimated Δd values. On the other hand, the values of k°_{max}/k_c and j_{cat} at the ME-functionalized Au electrode were larger than those obtained with the planar Au electrode. When it is assumed that the k_c value is equal at both electrodes, it can be concluded that k°_{max} and $\Gamma_{E,eff}$ increase due to modification of the Au electrodes with ME. In the case of FDH, the electrode modification affects not Δd but $\Gamma_{E,eff}$ [21]. The similar improvement in the DET-type bioelectrocatalysis by ME modification was explained by applying a surfactant bilayer model [10]. Briefly, the hydrophilic surface of the ME-functionalized electrode is favorable for forming the Triton® X-100 bilayer into which the enzymes are embedded, which increases $\Gamma_{E,eff}$ and shortens the distance between the electrode-active center of the enzyme and the electrode. Similar effects are expected in this case. However, further studies are required for in-depth discussion of how surface modification of the electrode affects the DET-type bioelectrocatalysis by AlDH.

3.2. Effects of CN^- on reverse DET-type bioelectrocatalysis by AlDH

We investigated the effects of CN^- on DET-type bioelectrocatalysis by AlDH. CN^- is known to be coordinated to the axial ligand of the heme iron, which results in a shift in the redox potential by approximately 0.4 V toward the negative direction [22]. After the addition of 1 mM potassium cyanide (KCN), a small bioelectrocatalytic wave of acetaldehyde oxidation at the AlDH-modified Au electrode was first observed, but the intensity of the wave gradually decreased with time and the signal finally disappeared (Fig. S4). The results can be explained by the following mechanisms:

1) The coordination of CN^- to the hemes *c* in AlDH and the adsorption of AlDH on an electrode proceed simultaneously, where the former is slower than the latter because the dissociation of a proton from HCN (pK_a = 9.2) is unfavorable under acidic conditions. (Caution: addition of KCN to acidic solutions must be performed with good ventilation as the process generates HCN).

2) Intramolecular electron transfer in AlDH is inhibited by CN^- coordination. This means that the electrons are transferred from the catalytic center to the electrode through one or more hemes *c* in the native enzyme.

Fig. 2 presents the schematics of the electron transfer pathway of AlDH. The approximated values of the formal potential at pH 4.0 were evaluated based on the following considerations: a) the $E^{\circ\prime}_E$ value of one of hemes *c* obtained in this work, b) the formal potential of the acetate/acetaldehyde redox couple ($E^{\circ\prime}_S$) is −0.78 V at pH 7.0 [23] and shifts by −89 mV pH^{-1} based on the following and the Nernst equations:

$$CH_3COO^- + 3H^+ + 2e^- \rightleftarrows CH_3CHO + H_2O \quad (4)$$

3) The formal potential of the Moco ($E^{\circ\prime}_{Moco}$) in AlDH is assumed to be close to that of xanthine oxidase (−0.5 V [24]), which is a typical molybdenum enzyme. The involvement of other electron-mediating redox centers was ignored here. The downhill property is well explained by electron transfer from acetaldehyde to the electrode-active heme *c* at pH 4.0. However, the CN^- coordination to the heme *c* results in an uphill barrier in the intramolecular electron transfer process, which inhibits the enzyme activity for acetaldehyde oxidation (Fig. 2A).

At lower pH (pH 2.5), $E^{\circ\prime}_S$ shifts toward positive potential and becomes more positive than E°_{Moco}. Therefore, it was expected that electron transfer from the CN^--coordinated heme *c* to acetate via Moco would be thermodynamically favorable, as shown in Fig. 2B. This hypothesis was tested by using a MWCNT-modified GC electrode as a platform for AlDH because the electrode provided a relatively smaller background current probably ascribed to proton reduction under strongly acidic conditions, compared to the planar Au and GC electrodes. In addition, DET-type bioelectrocatalytic acetaldehyde oxidation was observed at the AlDH-adsorbed MWCNT-modified GC electrodes, with a larger current density than that observed at AlDH-modified Au electrodes (Fig. S5). Since the AlDH solution at pH 2.5 kept the activity for acetaldehyde oxidation, there was no fatal change in the enzyme conformation under acidic conditions.

Fig. 3 shows the CVs recorded at the MWCNT-modified GC electrodes in an McB (pH 2.5) containing 0.1 M acetic acid and 1 mM KCN under anaerobic conditions. After addition of AlDH at a final concentration of 2 μg mL^{-1} into the electrolysis solution, the cathodic DET-type bioelectrocatalytic current for acetate reduction by CN^--coordinated AlDH was observed. An increase in the current was only observed in the presence of AlDH, KCN, and acetate. Here, it is noteworthy that the current density increased over many hours, as demonstrated by the multi-scanned CVs in Fig. S6. The current decrease in the first 2 h is plausibly due to adsorption of AlDH on the electrodes, and CN^- was gradually coordinated to AlDH, which seemed to proceed very slowly, as described above. Only the current decrease was observed in the absence of KCN (Fig. S7), which also supports the above process. In addition, the onset potential (approximately − 0.6 V) is somewhat more negative than that expected from the formal potential of the CN^--coordinated electrode-active heme *c*. The potential shift induced by CN^- coordination might be larger than 0.4 V. However, DET-type acetate reduction cannot be observed in the presence of high concentrations (~mM) of acetaldehyde (data not shown), which is suggested to be due to the biased catalytic property and the product inhibition.

Table 1
Refined parameters from non-linear regression analysis of voltammograms. The errors were evaluated from Student's *t*-distribution at a 90% confidence level (n = 5).

	$E^{\circ\prime}_E$ / mV	k°_{max}/k_c	Δd / Å	j_{cat} / μA cm^{-2}
AlDH-modified Au	−38 ± 6	90 ± 30	7.1 ± 0.8	20 ± 10
AlDH and ME-modified Au	−37 ± 1	500 ± 400	8.4 ± 0.9	30 ± 20

4. Conclusions

DET-type bioelectrocatalysis of acetaldehyde oxidation by AlDH

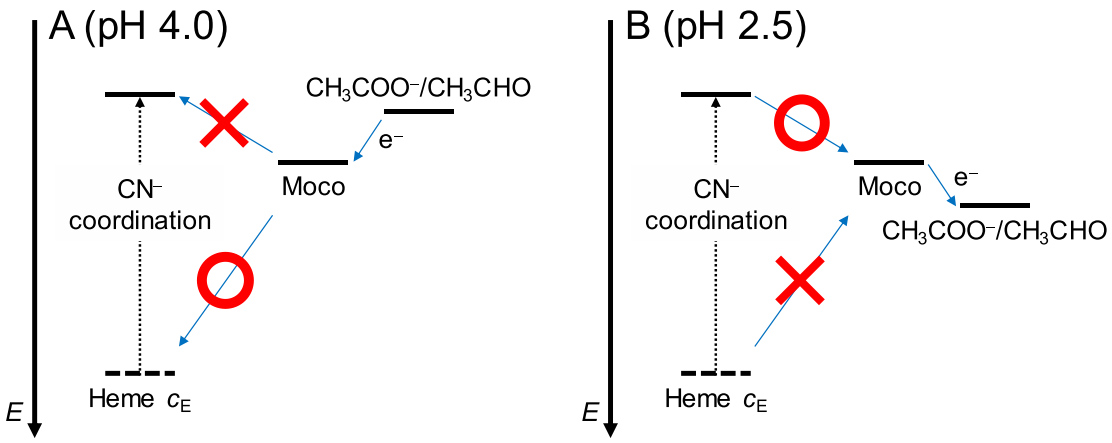

Fig. 2. Proposed potential profiles for acetaldehyde oxidation at pH 4.0 (A) and acetate reduction at pH 2.5 (B) in DET-type bioelectrocatalysis by AlDH. Heme c_E indicates the electrode-active heme *c*.

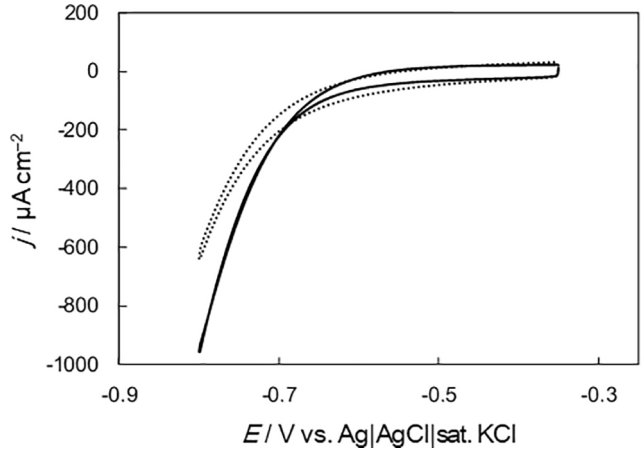

Fig. 3. CVs for acetate reduction at the AlDH-adsorbed MWCNT-modified GC electrode in an McB (pH 2.5) containing 0.1 M acetic acid and 1 mM KCN in the presence (solid line) and absence (dotted line) of 2 μg mL^{-1} AlDH at 25 °C under quiescent and anaerobic conditions, at $\nu = 10$ mV s^{-1}.

from *Gluconobacter oxydans* at several types of electrodes was examined, and the kinetics and thermodynamics of the bioelectrocatalytic reaction were evaluated. The effects of CN^- on the DET-type bioelectrocatalytic activity of AlDH were also evaluated, and the reverse DET-type bioelectrocatalytic activity of CN^--coordinated AlDH, i.e., acetate reduction, was observed under strongly acidic conditions. Further studies are required for detailed clarification of the characteristics of bioelectrocatalysis by AlDH. The reaction can be applied to detecting acetaldehyde in food and environment analyses, utilizing acetaldehyde as a biofuel, and producing acetic acid from acetaldehyde without any additional redox mediators.

CRediT authorship contribution statement

Taiki Adachi: Investigation, Conceptualization, Writing - original draft, Visualization. **Yuki Kitazumi:** Conceptualization. **Osamu Shirai:** Conceptualization, Writing - review & editing. **Kenji Kano:** Conceptualization, Writing - review & editing, Supervision, Project administration.

Declaration of Competing Interest

The authors declare that they have no known competing financial interests or personal relationships that could have appeared to influence the work reported in this paper.

Acknowledgements

We would like to thank Editage (www.editage.com) for English language editing.

Appendix A. Supplementary data

Supplementary data to this article can be found online at https://doi.org/10.1016/j.elecom.2020.106911.

References

[1] J. Tkac, J. Svitel, I. Vostiar, M. Navratil, P. Gemeiner, Membrane-bound dehydrogenases from *Gluconobacter* sp.: Interfacial electrochemistry and direct bioelectrocatalysis, Bioelectrochemistry 76 (1-2) (2009) 53–62, https://doi.org/10.1016/j.bioelechem.2009.02.013.
[2] T. Adachi, Y. Kaida, Y. Kitazumi, O. Shirai, K. Kano, Bioelectrocatalytic performance of D-fructose dehydrogenase, Bioelectrochemistry 129 (2019) 1–9, https://doi.org/10.1016/j.bioelechem.2019.04.024.
[3] T. Ikeda, D. Kobayashi, F. Matsushita, T. Sagara, K. Niki, Bioelectrocatalysis at electrodes coated with alcohol dehydrogenase, a quinohemoprotein with heme *c* serving as a built-in mediator, J. Electroanal. Chem. 361 (1-2) (1993) 221–228, https://doi.org/10.1016/0022-0728(93)87058-4.
[4] A. Ramanavicius, K. Habermüller, E. Csöregi, V. Laurinavicius, W. Schuhmann, Polypyrrole-entrapped quinohemoprotein alcohol dehydrogenase. Evidence for direct electron transfer via conducting-polymer chains, Anal. Chem. 71 (16) (1999) 3581–3586, https://doi.org/10.1021/ac981201c.
[5] J. Razumiene, M. Niculescu, A. Ramanavicius, V. Laurinavicius, E. Csöregi, Direct bioelectrocatalysis at carbon electrodes modified with quinohemoprotein alcohol dehydrogenase from *Gluconobacter sp.* 33, Electroanalysis 14 (2002) 43–49, https://doi.org/10.1002/1521-4109(200201)14:1<43::AID-ELAN43>3.0.CO;2-5.
[6] S. Tsujimura, T. Abo, Y. Ano, K. Matsushita, K. Kano, Electrochemistry of D-Gluconate 2-Dehydrogenase from *Gluconobacter frateurii* on Indium Tin Oxide Electrode Surface, Chem. Lett. 36 (9) (2007) 1164–1165, https://doi.org/10.1246/cl.2007.1164.
[7] B.L. Treu, S.D. Minteer, Isolation and purification of PQQ-dependent lactate dehydrogenase from *Gluconobacter* and use for direct electron transfer at carbon and gold electrodes, Bioelectrochemistry 74 (1) (2008) 73–77, https://doi.org/10.1016/j.bioelechem.2008.07.005.
[8] O. Adachi, K. Tayama, E. Shinagawa, K. Matsushita, M. Ameyama, Purification and characterization of membrane-bound aldehyde dehydrogenase from *Gluconobacter suboxydans*. Agric. Biol. Chem. 44 (3) (1980) 503–515, https://doi.org/10.1271/bbb1961.44.503.
[9] C. Prust, M. Hoffmeister, H. Liesegang, A. Wiezer, W.F. Fricke, A. Ehrenreich, G. Gottschalk, U. Deppenmeier, Complete genome sequence of the acetic acid bacterium *Gluconobacter oxydans*, Nat Biotechnol 23 (2) (2005) 195–200, https://doi.org/10.1038/nbt1062.
[10] S. Kawai, T. Yakushi, K. Matsushita, Y. Kitazumi, O. Shirai, K. Kano, Role of a non-ionic surfactant in direct electron transfer-type bioelectrocatalysis by fructose dehydrogenase, Electrochim. Acta 152 (2015) 19–24, https://doi.org/10.1016/j.electacta.2014.11.113.

[11] P. Bollella, E. Katz, Bioelectrocatalysis at carbon nanotubes, Methods Enzymol. 630 (2020) 215–247, https://doi.org/10.1016/bs.mie.2019.10.012.
[12] I. Mazurenko, A. de Poulpiquet, E. Lojou, Recent developments in high surface area bioelectrodes for enzymatic fuel cells, Curr. Opin. Electrochem. 5 (1) (2017) 74–84, https://doi.org/10.1016/j.coelec.2017.07.001.
[13] Y.u. Sugimoto, R. Takeuchi, Y. Kitazumi, O. Shirai, K. Kano, Significance of Mesoporous Electrodes for Noncatalytic Faradaic Process of Randomly Oriented Redox Proteins, J. Phys. Chem. C 120 (46) (2016) 26270–26277, https://doi.org/10.1021/acs.jpcc.6b07413.s001.
[14] Y. Sugimoto, Y. Kitazumi, O. Shirai, K. Kano, Effects of mesoporous structures on direct electron transfer-type bioelectrocatalysis: facts and simulation on a three-dimensional model of random orientation of enzymes, Electrochemistry 85 (2) (2017) 82–87, https://doi.org/10.5796/electrochemistry.85.82.
[15] Y. Kitazumi, O. Shirai, M. Yamamoto, K. Kano, Numerical simulation of diffuse double layer around microporous electrodes based on the Poisson–Boltzmann equation, Electrochim. Acta 112 (2013) 171–175, https://doi.org/10.1016/j.electacta.2013.08.117.
[16] H. Habe, Y. Shimada, T. Yakushi, H. Hattori, Y. Ano, T. Fukuoka, D. Kitamoto, M. Itagaki, K. Watanabe, H. Yanagishita, K. Matsushita, K. Sakaki, Microbial Production of Glyceric Acid, an Organic Acid That Can Be Mass Produced from Glycerol, AEM 75 (24) (2009) 7760–7766, https://doi.org/10.1128/AEM.01535-09.
[17] H.-q. Xia, Y. Kitazumi, O. Shirai, K. Kano, Enhanced direct electron transfer-type bioelectrocatalysis of bilirubin oxidase on negatively charged aromatic compound-modified carbon electrode, J. Electroanal. Chem. 763 (2016) 104–109, https://doi.org/10.1016/j.jelechem.2015.12.043.
[18] C. Léger, A.K. Jones, S.P.J. Albracht, F.A. Armstrong, Effect of a Dispersion of Interfacial Electron Transfer Rates on Steady State Catalytic Electron Transport in [NiFe]-hydrogenase and Other Enzymes, J. Phys. Chem. B 106 (50) (2002) 13058–13063, https://doi.org/10.1021/jp0265687.
[19] C.C. Moser, J.M. Keske, K. Warncke, R.S. Farid, P.L. Dutton, Nature of biological electron transfer, Nature 355 (6363) (1992) 796–802, https://doi.org/10.1038/355796a0.
[20] S. Kawai, T. Yakushi, K. Matsushita, Y. Kitazumi, O. Shirai, K. Kano, The electron transfer pathway in direct electrochemical communication of fructose dehydrogenase with electrodes, Electrochem. Commun. 38 (2014) 28–31, https://doi.org/10.1016/j.elecom.2013.10.024.
[21] H.-q. Xia, Y. Hibino, Y. Kitazumi, O. Shirai, K. Kano, Interaction between D-fructose dehydrogenase and methoxy-substituent-functionalized carbon surface to increase productive orientations, Electrochim. Acta 218 (2016) 41–46, https://doi.org/10.1016/j.electacta.2016.09.093.
[22] I. Taniguchi, Y. Mie, K. Nishiyama, V. Brabec, O. Novakova, S. Neya, N. Funasaki, Electrochemistry of monoazahemin reconstituted myoglobin at an indium oxide electrode, J. Electroanal. Chem. 420 (1-2) (1997) 5–9, https://doi.org/10.1016/S0022-0728(96)01022-4.
[23] P.A. Loach, Physical and chemical data, Vol. I, in: G.D. Fasman (Ed.), Handbook of biochemistry and molecular biology, 3rd ed., CRC Press, Cleveland, 1976, pp. 123–130.
[24] K. Kano, Redox potentials of proteins and other compounds of bioelectrochemical interest in aqueous solutions, Rev. Polarogr. 48 (1) (2002) 29–46, https://doi.org/10.5189/revpolarography.48.29.